Magnetic and noncentrosymmetric Weyl fermion semimetals in the RAlGe family of compounds (R=rareearth)

Guoqing Chang, Bahadur Singh, Su-Yang Xu, Guang Bian, Shin-Ming Huang, Chuang-Han Hsu, Ilya Belopolski, Nasser Alidoust, Daniel S. Sanchez, Hao Zheng, Hong Lu, Xiao Zhang, Yi Bian, Tay-Rong Chang, Horng-Tay Jeng, Arun Bansil, Han Hsu, Shuang Jia, Titus Neupert, Hsin Lin, and M. Zahid Hasan

Phys. Rev. B **97**, 041104 — Published 9 January 2018

DOI: 10.1103/PhysRevB.97.041104

Magnetic and noncentrosymmetric Weyl fermion semimetals in the RAlGe family of compounds (R=rare earth)

Guoqing Chang*,[1,2] Bahadur Singh*,[1,2] Su-Yang Xu*†,[3] Guang Bian,[3,4] Shin-Ming Huang,[5] Chuang-Han Hsu,[1,2] Ilya Belopolski,[3] Nasser Alidoust,[3] Daniel S. Sanchez,[3] Hao Zheng,[3,6] Hong Lu,[7] Xiao Zhang,[7] Yi Bian,[7] Tay-Rong Chang,[8,9] Horng-Tay Jeng,[8,10] Arun Bansil,[11] Han Hsu,[12] Shuang Jia,[7,13] Titus Neupert,[14,15] Hsin Lin†,[1,2,10] and M. Zahid Hasan †[3,16]

[1]*Centre for Advanced 2D Materials and Graphene Research Centre National University of Singapore, 6 Science Drive 2, Singapore 117546*
[2]*Department of Physics, National University of Singapore, 2 Science Drive 3, Singapore 117542*
[3]*Laboratory for Topological Quantum Matter and Spectroscopy (B7), Department of Physics, Princeton University, Princeton, New Jersey 08544, USA*
[4]*Department of Physics and Astronomy, University of Missouri, Columbia, Missouri 65211, USA*
[5]*Department of Physics, National Sun Yat-sen University, Kaohsiung 804, Taiwan*
[6]*School of Physics and Astronomy, Shanghai Jiao Tong Univeristy, 200240 shanghai, China.*
[7]*International Center for Quantum Materials, School of Physics, Peking University, China*
[8]*Department of Physics, National Tsing Hua University, Hsinchu 30013, Taiwan*
[9]*Department of Physics, National Cheng Kung University, Tainan 701, Taiwan*
[10]*Institute of Physics, Academia Sinica, Taipei 11529, Taiwan*
[11]*Department of Physics, Northeastern University, Boston, Massachusetts 02115, USA*
[12]*Department of Physics, National Central University, Jhongli City, Taoyuan 32001, Taiwan*
[13]*Collaborative Innovation Center of Quantum Matter, Beijing,100871, China*
[14]*Princeton Center for Theoretical Science, Princeton University, Princeton, New Jersey 08544, USA*
[15]*Department of Physics, University of Zurich, Winterthurerstrasse 190, 8057 Zurich, Switzerland*
[16]*Princeton Institute for Science and Technology of Materials, Princeton University, Princeton, New Jersey, 08544, USA*

Weyl semimetals are novel topological conductors that host Weyl fermions as emergent quasiparticles. In this paper, we propose a new type of Weyl semimetal state that breaks both time-reversal symmetry and inversion-symmetry in the RAlGe (R=Rare earth) family. Compared to previous predictions of magnetic Weyl semimetal candidates, the prediction of Weyl nodes in RAlGe are more robust and less dependent on the details of the magnetism, because the Weyl nodes are already generated by the inversion breaking and the ferromagnetism acts as a simple Zeeman coupling that shifts the Weyl nodes in k space. Moreover, RAlGe offers remarkable tunability, which covers all varieties of Weyl semimetals including type-I, type-II, inversion-breaking and time-reversal breaking, depending on a suitable choice of the rare earth elements. Further, the unique noncentrosymmetric and ferromagnetic Weyl semimetal state in RAlGe enables the generation of spin-currents.

Finding new quantum materials with useful properties is one of the frontiers of modern condensed matter physics and material science [1–6]. The recent realization of nonmagnetic Weyl semimetal state in the TaAs class of materials [7–25], has attracted significant attention. Further transport measurements have revealed unconventional magnetic and optical responses of TaAs family [26–29]. Despite recent advances of topological semimetals in both theory[30–43] and experiment [26–29, 44–51] , the ferromagnetic Weyl semimetal [8, 9, 52–57] has not been realised in experiments. A key issue is that first-principles band structure calculations on these magnetic materials (e.g. iridates [8] and $HgCr_2Se_4$ [52]) are quite challenging. For example, the all-in (all-out) magnetic structure in iridates appeared to be complicated to verify in experiments [53] and model in first-principles calculations [8, 54]. Also, for many magnetic materials such as $HgCr_2Se_4$ the magnetic band structure may be very sensitive to the details of the magnetism. As a result, the first-principles prediction of Weyl nodes in magnetic compounds is not as robust as that of in nonmagnetic compounds such as TaAs [10, 11]. Here, we propose a new strategy to search for magnetic Weyl semimetals. Taking advantage of the Weyl nodes generated by inversion-symmetry breaking in the nonmagnetic compound LaAlGe [44, 58], we present a new type of magnetic Weyl semimetal in its iso-structural sister compounds CeAlGe and PrAlGe [59, 60] that are ferromagnetic [61–63]. We show that the ferromagnetism in RAlGe can be more reliably modeled in first-principles calculation as it is found to not completely change the band structure. Rather, it acts as a Zeeman coupling and splits the spin-up and spin-down bands, which shifts the Weyl nodes in k space to break time-reversal symmetry. For these reasons, the prediction of Weyl nodes in RAlGe are less dependent on the details of the magnetism. Moreover, we show that the RAlGe family offers remarkable tunability, where type-I, type-II [30], inversion breaking, and time-reversal breaking types of Weyl semimetal states are all available. Further, as re-

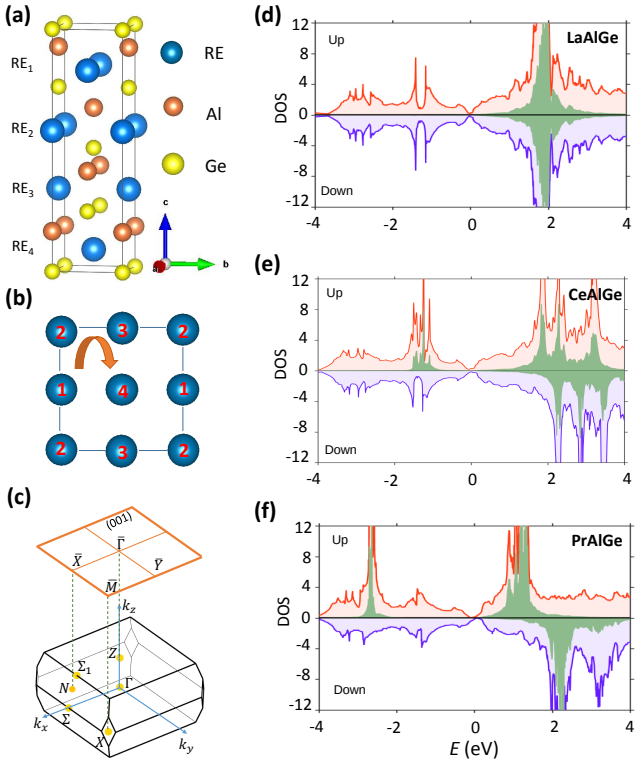

FIG. 1. Lattice structure, Brillouin zone and density of state (DOS) of RAlGe (R=La, Ce, and Pr). (a) Body-centered tetragonal structure of RAlGe, with space group $I4_1md$ (109). The structure consists of stacks of rare earth element (RE), Al, and Ge layers and along the (001) direction each layer consists of only one type of elements. (b) The schematic of RE atomic layer showing the skew axis along the c axis. (c) The bulk and (001) surface Brillouin zone (BZ). (d-f) First-principles DOS of LaAlGe (d), CeAlGe (e) and PrAlGe (f). The partial DOS for spin-up and spin-down states are plotted in red and violet colors, respectively. The DOS from localized f orbitals are drawn in green color.

cently predicted in theory [64], the time-reversal and inversion breaking Weyl semimetals can uniquely induce a quantum spin current without a concomitant charge current. In addition, while a noncentrosymmetric (magnetic) Weyl semimetal is an intermediate phase between a trivial insulator and a 3D topological insulator (3D stacked Chern insulator) state [65], here, with both symmetries broken, the phase diagram may be even richer. This rich phase diagram may be potentially explored via doping or chemical substitution.

RAlGe crystallizes in a body-centered tetragonal Bravais lattice with a $\mathcal{I}$-breaking space group $I4_1md$ (109) [58–60] (Figures. 1(a,b)). Our results show that LaAlGe is nonmagnetic, whereas CeAlGe and PrAlGe are ferromagnetic with their magnetization easy axse along the a and c directions, representively. For CeAlGe, the calculated magnetic moment is 1 μ_B per Ce atom and the experimental measured value is 0.94 μ_B [61]. For PrAlGe, the calculated magnetic moment is 2 μ_B per Pr atom whereas the experimental value has not been reported in literature. Figs. 1(d,e,f) show the calculated density of states (DOS) without spin-orbit coupling (SOC) for RAlGe. The DOS of the majority and minority spin states are colored in red and blue. It can be seen clearly that in LaAlGe the DOS of the two spins are equal, consistent with its nonmagnetic nature. In contrast, an imbalance between the DOS of the majority and minority spin states is seen in CeAlGe and PrAlGe, suggesting a ferromagnetic ground state in agreement with the experimental finding [62, 63]. The green shaded areas are the DOS of $f$electrons. The electronic configuration of La atom is [Xe]$6s^25d^14f^0$, meaning that all f orbitals are empty. Indeed, Fig. 1(d) shows that the all f electrons are in the conduction bands. On the other hand, a Ce (or Pr) atom should have 1 (or 2) electrons occupying the f orbitals. As a result, we see some f bands below the Fermi level in Figs. 1(e,f). Moreover, our calculations (Figs. 1(e,f)) show that the occupied f electron states in CeAlGe and PrAlGe are clearly spin-polarized. These results suggest that the ferromagnetic coupling between the f electrons' local moments lead to ferromagnetism in CeAlGe and PrAlGe, which, in turn, makes the conduction electrons (s, p, d orbitals) near the Fermi level also spin-polarized. Furthermore, our band structure calculations without SOC (Figs. 2(c,e)) clearly show a spin splitting in the electronic states. These results confirm our conceptual picture: The ferromagnetism arises from the ordering of the f electrons' local moments. These local moments serve as an effective Zeeman field and make the conduction (s, p, d orbital) bands spin polarized. We highlight the fact that the ferromagnetism can be treated as a Zeeman coupling and does not completely change the band structure at low-energy. In the presence of SOC, the spin-up and spin-down states are further mixed by Rashba/Dresselhaus interactions due to the lack of inversion symmetry, making spin not a good quantum number. Thus, we do not color code the bands in Figs. 2(d,f).

In order to explain the Weyl nodes in CeAlGe and PrAlGe, we start from the nonmagnetic compound LaAlGe. In the absence of spin-orbit coupling, the crossing between conduction and valence bands yields four nodal lines, on the $k_x = 0$ and $k_y = 0$ mirror planes and also 4 pairs of (spinless) Weyl nodes on the $k_z = 0$ plane, which we denoted as W3 [44]. Upon the inclusion of the spin-orbit coupling, the nodal lines are gapped out and 24 Weyl nodes emerge in the vicinity. We refer to the 8 Weyl nodes located on the $k_z = 0$ plane as W1 and the remaining 16 Weyl nodes away from this plane as W2 [44]. Moreover, each W3 (spinless) Weyl node splits into two (spinful) Weyl nodes of the same chirality, which we call W3' and W3" [44]. Hence, in total there are 40 Weyl nodes for LaAlGe [44].

We now turn to the Weyl semimetal states in CeAlGe and PrAlGe. We conceptually consider a temperature dependent evolution. Starting at a higher temperature

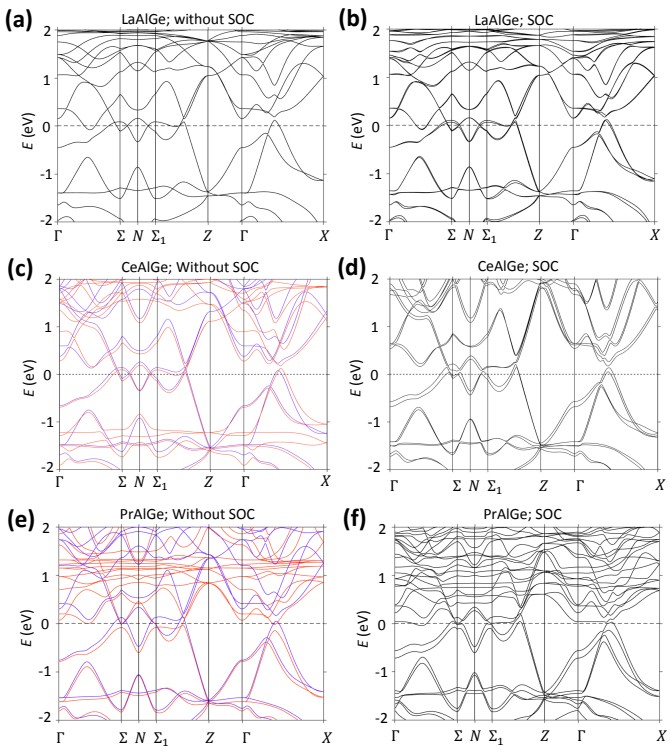

FIG. 2. First-principles band structure of RAlGe (R=La, Ce, and Pr). (a,b) Calculated bulk band structure of LaAlGe without and with the inclusion of spin-orbit coupling. (c,d) Bulk band structure of CeAlGe without and with the inclusion of spin-orbit coupling. In c the bands of spin-up and spin-down states are plotted in red and violet colors, respectively. (e,f) same as (c,d) but for PrAlGe.

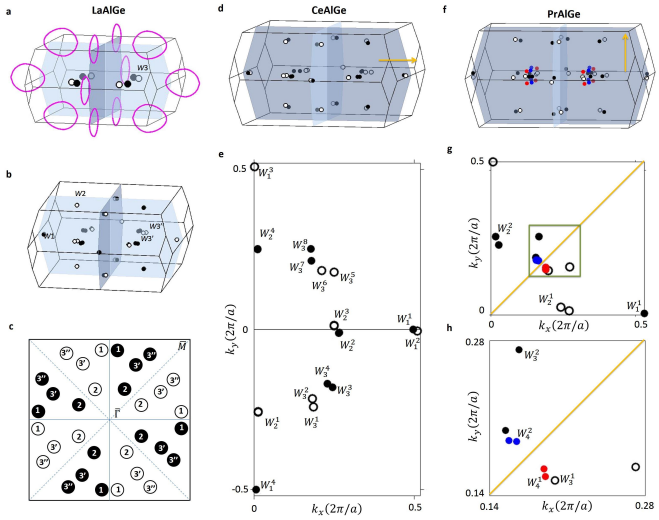

FIG. 3. Weyl fermions in LaAlGe, CeAlGe, and PrAlGe. (a), (c) Weyl nodes (denoted by W3) in the first BZ of CeAlGe and PrAlGe with SOC. The arrows indicate the magnetization orientation. The red and blue dots denote the new Weyl nodes (W4) generated by the magnetization of f orbitals of Pr. (b) Projection of the Weyl nodes on the (001) surface Brillouin zone (SBZ) of CeAlGe. The configuration of the other half of the SBZ can be obtained by considering mirror symmetry. (d), (e) Same as b but for PrAlGe. (f-h) Schematic illustrations of the band dispersion of Weyl fermions in LaAlGe, CeAlGe, and PrAlGe, respectively.

above the Curie transition, we expect the Ce(Pr)AlGe sample to already become a Weyl semimetal because of the broken space-inversion symmetry with 40 Weyl nodes as in LaAlGe. Now we lower the temperature below the Curie temperature, the effect of the ferromagnetism in CeAlGe and PrAlGe can be understood qualitatively as a Zeeman coupling to the conduction electron states. To the lowest order, we expect that this will shift the Weyl nodes in a way that their momentum space configuration reflects the time-reversal symmetry breaking. We use this picture to understand the calculated results of the Weyl nodes configuration of these two compounds. In CeAlGe, indeed, we found that the Weyl nodes are still the W1, W2, and W3 as in LaAlGe (Fig. 3(a, b)). The difference is that they are shifted away from the original location due to magnetism. In LaAlGe all W1 nodes can be related by symmetry operations. However, in CeAlGe, the inclusion of a magnetization along a direction gives rise to 4 inequivalent W1 Weyl nodes. They have different momentum space locations and energies. Similarly, there are now 4 inequivalent W2 and 8 inequivalent W3 Weyl nodes in CeAlGe because of the reduction of symmetries by the inclusion of the magnetization. In PrAlGe, the magnetization along the c axis leads to 1 inequivalent W1, 2 inequivalent W2 and 2 inequivalent W3 Weyl nodes. In addition, we find that the inclusion of ferromagnetization in PrAlGe may introduce new Weyl nodes, which we denote as the W4 nodes (Figs. 3(c-e)). The chiral charges of Weyl points in RAlGe are determined by the net Berry flux passing through the 2D manifold that enclosing Weyl fermions[8].

In order to understand how the Weyl nodes are shifted by the magnetization, we discuss the symmetry constraints in the presence of the ferromagnetic order in CeAlGe and PrAlGe.

In CeAlGe, the magnetization is oriented along a axis. Both $\mathcal{T}$ and C_2 reverse this in-plane magnetization. However, their product $C_2\mathcal{T}$ is still a symmetry of the magnetic system and the same is true for M_x. Thus, all symmetry-nonequivalent Weyl nodes are found in the $k_x > 0$ part of the BZ depicted in Fig. 3(b). Due to $C_2\mathcal{T}$, all W1- and W3-derived Weyl nodes are still pinned to $k_z = 0$ and the W2-derived nodes are found in $\pm k_z$ pairs. It is also interesting to notice that the movement of the all Weyl nodes in the vicinity of the M_y ($//k_x$) mirror plane (W_1^1, W_1^2, W_2^2, and W_2^3), is much more sig-

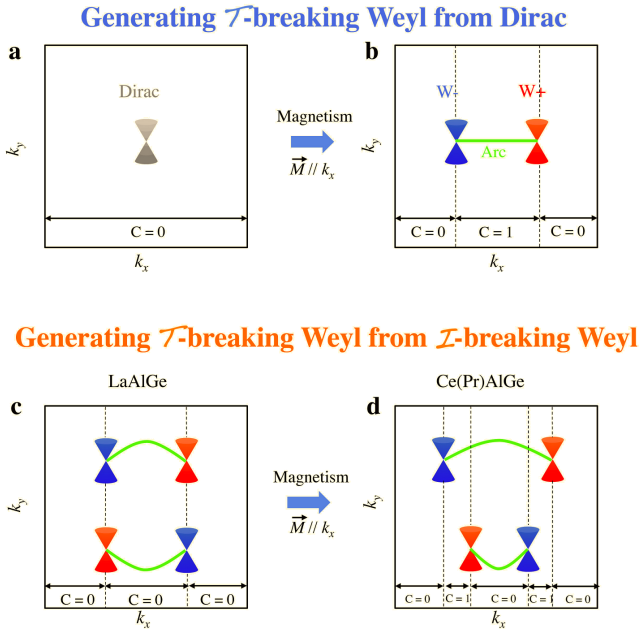

FIG. 4. A new route to generating magnetic Weyl fermions. (a,b,) The Dirac node in a Dirac semimetal splits into a pair of Weyl nodes upon the inclusion of a magnetic field. The Weyl nodes are connected by a Fermi arc surface state. (c,d,) Two pairs of Weyl nodes are present in a inversion-breaking Weyl semimetal. The Weyl nodes are shifted in momentum space upon the inclusion of a magnetic field, generating regions in $\boldsymbol{k}$ space with a non-zero Chern number.

nificant than those of the M_x ($//k_y$) mirror plane (W_1^3, W_1^4, W_2^1, and W_2^4). This phenomenon is also symmetry related. Specifically, the Weyl nodes near the M_x ($//k_y$) mirror plane are roughly stationary upon magnetization because the symmetries $C_2\mathcal{T}$ and M_x are the only constraints to the effective Hamiltonian near the M_x mirror plane [10, 11]. However, this term turns out to be only relevant for the energy but not for the position of the Weyl nodes. The detailed information of the Weyl nodes including the momentum space locations, the energies and the type, is shown in the Supplemental Material, Sec. C [68] .

In PrAlGe, the magnetization is oriented along z. Both $\mathcal{T}$ and any of the mirror and glide mirror symmetries reverse this magnetization. However, their products, e.g., $\mathcal{T}M_x$, are still a symmetry of the magnetic system. Furthermore, C_{2z} and $\bar{C}_{4z}$ are preserved by the magnetization. Thus, all symmetry-nonequivalent Weyl nodes are found in a quadrant of the BZ depicted in Fig. 3(d). The main difference to LaAlGe is that $C_{2z}\mathcal{T}$ symmetry is broken. As a result, we expect the W1 and W3 Weyl nodes to move along the k_z direction and become no longer pinned to $k_z = 0$. On the other hand, the W2 Weyl nodes are expected to stop appearing in $\pm k_z$ pairs.

Our theoretical discovery of CeAlGe and PrAlGe reveals a new route to realizing $\mathcal{T}$-breaking Weyl fermions. The traditional and commonly accepted proposal for realizing $\mathcal{T}$-breaking Weyl fermions is to break time-reversal symmetry of a 3D Dirac fermion system, as shown in Figs. 4(a,b). In this way, the Weyl fermions actually arise from the breaking of time-reversal symmetry. We can qualitatively understand the anomalous Hall effect. As shown in Fig. 4(b), we consider the Chern number of a series of (k_y, k_z) 2D slices at different k_x-intercepts. Any slice between the left boundary of the BZ and the first dotted line has a Chern number of 0. As we continue sweeping the (k_y, k_z) slice to the right, we pass through the blue Weyl node and therefore the Chern number changes by 1. Consequently, a slice between the first dotted line and the second dotted line has a Chern number of 1. Then we pass the red Weyl node and the Chern number of a slice between the second dotted line and the right boundary of the BZ is 0. As a result, the Chern number averaged over all k_z in the BZ is nonzero, which demonstrates the existence of an anomalous Hall effect. It can be checked that this simple consideration carries over to CeAlGe and PrAlGe, despite the presence of additional symmetries, and an anomalous Hall effect is expected in the plane perpendicular to the respective magnetization. By contrast, in the Dirac semimetal case in Fig. 4(a), the Chern number of any slice is zero, consistent with the fact that Dirac semimetals do not show anomalous Hall conductance. In terms of experimental realization, this proposal means that one needs to introduce magnetism to a Dirac semimetal system such as $TlBi(S_{1-x}Se_x)_2$, Cd_3As_2 and Na_3Bi. Since these materials are nonmagnetic, one will need to dope the system with magnetic dopants, which has been proven to be quite difficult. It is also challenging to systematically study the band structure of the magnetically doped system through first-principles calculations.

We now elaborate on our new route to realizing $\mathcal{T}$-breaking Weyl fermions as demonstrated in CeAlGe and PrAlGe. Rather than starting from a Dirac semimetal, we start from a space-inversion ($\mathcal{I}$) breaking Weyl semimetal. As schematically shown in Fig. 4(c), two pairs of Weyl nodes are generated by the breaking of space inversion symmetry. In this case, magnetization is only responsible for shifting the momentum space location of the Weyl nodes. We note that a $\mathcal{T}$-breaking Weyl semimetal is defined as the breaking of time-reversal symmetry in terms of the Weyl node configuration. Specifically, Weyl nodes of same chirality cannot appear at opposite momenta ($\pm\vec{k}$). Therefore, although in this case the Weyl fermions do not arise from ferromagnetism, the system in Fig. 4(d) still counts as a $\mathcal{T}$-breaking Weyl semimetal. This can also be seen by studying the Chern number of the (k_y, k_z) 2D slices. As shown in Figs. 4(c,d), introducing magnetism leads to a finite k_x range at which the Chern number of the (k_y, k_z) 2D slice is nonzero. This also suggests the existence of anomalous Hall conductance in the system shown in Fig. 4(d). We emphasize

a number of advantages of this new route. Introducing magnetism is done by going from LaAlGe to CeAlGe or PrAlGe rather than doping. This not only avoids the complicated doping processes, but also enables to systematically understand the band structure in calculations as we have achieved here. Furthermore, our results demonstrate an entirely new way to search for $\mathcal{T}$-breaking Weyl semimetals in future, i.e., to look for the iso-chemical ferromagnetic cousin compounds of an $\mathcal{I}$-breaking Weyl semimetal.

Finally, we highlight the tunability of the RAlGe family. As we have shown here, the low-energy band structures of LaAlGe, CeAlGe and PrAlGe realize the $\mathcal{I}$-breaking type-II, the $\mathcal{T}$-breaking type-II, and the $\mathcal{T}$-breaking type-I Weyl fermions. Moreover, n (electron) doping can be achieved by changing the ratio between Al and Ge, i.e., $RAl_{1-x}Ge_{1+x}$ [60]. In the weak disorder limit ($x \ll 1$), which cannot localize the conduction electorns from the Weyl fermions [66, 67], the doping will enable one to access other Weyl nodes that are above the Fermi level (Figs. 3(f-h)). In general, RAlGe is an extremely rich system that enables one to systematically study all types of Weyl fermions in a single family.

Work at Princeton was supported by the US Department of Energy under Basic Energy Sciences (Grant No. DOE/BES DE-FG-02-05ER46200). M.Z.H. acknowledges Visiting Scientist support from Lawrence Berkeley National Laboratory, and partial support from the Gordon and Betty Moore Foundation for theoretical work. The work at the National University of Singapore was supported by the National Research Foundation, Prime Minister's Office, Singapore under its NRF fellowship (NRF Award No. NRF-NRFF2013-03). S. J.acknowledge support by National science foundation of china No.11774007 and National Basic Research Program of China Grant No. 2014CB239302. The work at Northeastern University was supported by the US Department of Energy (DOE), Office of Science, Basic Energy Sciences grant number DE-FG02-07ER46352, and benefited from Northeastern University's Advanced Scientific Computation Center (ASCC) and the NERSC supercomputing center through DOE grant number DE-AC02-05CH11231. T.N. acknowledge support by the Swiss National Science Foundation (grant number 200021-169061) and the ERC-StG-Neupert-757867-PARATOP, respectively. The work at the National Sun Yat-sen University was supported by the Ministry of Science and Technology in Taiwan under Grant No. MOST105-2112-M110-014-MY3. T.-R.C. and H.-T. J are supported by the Ministry of Science and Technology. T.-R. C is supported by National Cheng Kung University. T.-R.C. and H.-T.J. also thank the National Center for Theoretical Sciences (NCTS) for technical support.

G.C., B.S., and S.-Y.X. contribute equally to this work.

[1] M. Z. Hasan, C. L. Kane, Rev. Mod. Phys. **82**, 3045 (2010).
[2] X.-L. Qi, S.-C. Zhang, Rev. Mod. Phys. **83**, 1057 (2011).
[3] M. Z. Hasan, S.-Y. Xu, M. Neupane, Topological Insulators, Topological semimetals, Topological Crystalline Insulators, and Topological Kondo Insulators. in *in Topological Insulators: Fundamentals and Perspectives* edited by F. Ortmann, S. Roche, S. O. Valenzuela (John Wiley & Sons, 2015).
[4] M. Z. Hasan, S.-Y. Xu, G. Bian, Phys. Scr. **T164**, 014001 (2015).
[5] M. Z. Hasan, S.-Y. Xu, I. Belopolski, and S.-M. Huang, 282 Annu. Rev. Condens. Matter Phys. **8**, 289 (2017).
[6] A. Bansil, H. Lin, and T. Das, Rev. Mod. Phys. **88**, 021004 (2016).
[7] H. Weyl, Z. Phys. **56**, 330-352 (1929).
[8] X. Wan, A. M. Turner, A. Vishwanath, S. Y. Savrasov, Phys. Rev. B **83**, 205101 (2011).
[9] A. A. Burkov, L. Balents, Phys. Rev. Lett. **107**, 127205 (2011).
[10] S.-M. Huang, S.-Y. Xu, I. Belopolski, C-C. Lee, G. Chang, B. Wang, N. Alidoust, G. Bian, M. Neupane, C. Zhang, S. Jia, A. Bansil, H. Lin, and M. Z. Hasan, Nat. Commun. **6**, 7373 (2015).
[11] H. Weng, C. Fang, Z. Fang, A. Bernevig, X. Dai, Phys. Rev. X **5**, 011029 (2015).
[12] S.-Y. Xu, I. Belopolski, N. Alidoust, M. Neupane, G. Bian, C. Zhang, R. Sabkar, G. Chang, Z. Yuan, C-C. Lee, S.-M. Huang, H. Zheng, J. Ma, D. S Sanchez, B. Wangm A. Bansil. F. Chou, P. P Shibayev, H. Lin, S. Jia, and M. Z. Hasan, Science **349**, 613 (2015).
[13] L. Lu, Z. Wang, D. Ye, L. Ran, L. Fu, J. D. Joannopoulos, and M. Soljačić, Science **349**, 622 (2015).
[14] B. Q. Lv, H. Weng, B. B. Fu, X. P. Wang, H. Miao, J. Ma, P. Richard, X. C. Huang, L. X. Zhao, G. F. Chen, Z. Fang, X. Dai, T. Qian, and H. Ding, Phys. Rev. X **5**, 031013 (2015).
[15] S.-Y. Xu, N. Alidoust, I. Belopolski, Z. Yuan, G. Bian, T.-R. Chang, H. Zheng, V. N Strocov, D. S. Sanchez, G. Chang, C. Zhang, D. Mou, Y. Wu, L. Huang, C-C. Lee, S.-M. Huang, B. Wang, A. Bansil, H.-T. Jeng, T. Neupert, A. Kaminski, H. Lin, S. Jia, and M. Z. Hasan, Nat. Phys. **11**, 748 (2015).
[16] L. X. Yang, Z. K. Liu, Y. Sun, H. Peng, H. F. Yang, T. Zhang, B. Zhou, Y. Zhang, Y. F. Guo, M. Rahn, D. Prabhakaran, Z. Hussain, S.-K. Mo, C. Felser, B. Yan and Y. L. Chen, Nat. Phys. **11**, 728 (2015).
[17] B. Q. Lv, N. Xu, H. M. Weng, J. Z. Ma, P. Richard, X. C. Huang, L. X. Zhao, G. F. Chen, C. E. Matt, F. Bisti, V. N. Strocov, J. Mesot, Z. Fang, X. Dai, T. Qian, M. Shi and H. Ding, Nat. Phys. **11**, 724 (2015).
[18] S.-Y. Xu, I. Belopolski, D. S. Sanchez, C. Zhang, G. Chang, C. Guo, G. Bian, Z. Yuan, H. Lu, T.-R. Chang, P. P. Shibayev, M. L. Prokopovych, N. Alidoust, H. Zheng, C.-C. Lee, S.-M. Huang, R. Sankar, F. Chou, C.-H. Hsu, H.-T. Jeng, A. Bansil, T. Neupert, V. N. Strocov, H. Lin, S. Jia and M. Z. Hasan, Science Advances, **1** , e1501902 (2015).
[19] H. Zheng, S.-Y. Xu, G. Bian, C. Guo, G. Chang, D. S. Sanchez, I. Belopolski, C.-C. Lee, S.-M. Huang, X. Zhang, R. Sankar, N. Alidoust, T.-R. Chang, F. Wu, T.

Neupert, F. Chou, H.-T. Jeng, N. Yao, A. Bansil, S. Jia, H. Lin and M. Z. Hasan, ACS nano **10**, 1378 (2016).
[20] H. Inoue, A. Gyenis, Z. Wang, J. Li, S. W. Oh, S. Jiang, N. Ni, B. A. Bernevig, A. Yazdani, Science, **351**, 1184 (2016).
[21] H. B. Nielsen, M. Ninomiya, Phys. Lett. B, **130**, 389 (1983).
[22] S. A. Parameswaran, T. Grover, D. A. Abanin, D. A. Pesin, and A. Vishwanath, Phys. Rev. X **4**, 031035 (2014).
[23] A. C. Potter, I. Kimchi, A. Vishwanath, Nat. Commun. **5**, 5161 (2014).
[24] Y. Baum, E. Berg, S. A. Parameswaran, A. Stern, Phys. Rev. X **5**, 041046 (2015).
[25] A. A. Zyuzin, A. A. Burkov, Phys. Rev. B **86**, 115133 (2012).
[26] X. Huang, L. Zhao, Y. Long, P. Wang, D. Chen, Z. Yang, H. Liang, M. Xue, H. M. Weng, Z. Fang, X. Dai, and G. Chen, Phys. Rev. X **5**, 031023 (2015).
[27] C. L. Zhang, S.-Y. Xu, I. Belopolski, Z. Yuan, Z. Lin, B. Tong, G. Bian, N. Alidoust, C-C. Lee, S.-M. Huang, T.-R. Chang, G. Chang, C-H. Hsu, H.-T. Jeng, M. Neupane, D. S. Sanchez, H. Zheng, J. Wang, H. Lin, C. Zhang, H.-Z. Lu, S.-Q. Shen, T. Neupert, M. Z. Hasan, and S. Jia, Nat. Commun. **7**, 10735 (2016).
[28] Q. Ma, S.-Y. Xu, C.-K. Chan, C.-L. Zhang, G. Chang, Y. Lin, W. Xie, T. Palacios, H. Lin, S. Jia, P. A. Lee, P. Jarillo-Herrero and N. Gedik, Nat. Phys. **13**, 842 (2017).
[29] C. L. Zhang, S.-Y. Xu, C. M. Wang, Z. Lin, Z. Z. Du, C. Guo, C-C. Lee, H. Lu, Y. Feng, S.-M. Huang, G. Chang, C.-H. Hsu, H. Liu, H. Lin, L. Li, C. Zhang, J. Zhang, X.-C. Xie, T. Neupert, M. Z. Hasan, H-Z. Lu, J. Wang, and S. Jia, Nat. Phys. **13**, 979 (2017).
[30] A. A. Soluyanov, D. Gresch, Z. Wang, Q. Wu, M. Troyer, X. Dai and B. A. Bernevig, Nature **527**, 495 (2015).
[31] G. Chang, D. S. Sanchez, B. J. Wieder, S.-Y Xu, F. Schindler, I. Belopolski, S.-M. Huang, B. Singh, D. Wu, T. Neupert, T.-R. Chang, H. Lin, and M. Z. Hasan, https://arxiv.org/abs/1611.07925 (2016).
[32] Y. Sun, S.-C. Wu, M. N. Ali, C. Felser, and B. Yan, Phys. Rev. B **92**, 161107 (2015).
[33] T.-R. Chang, S.-Y. Xu, G. Chang, C.-C. Lee, S.-M. Huang, B. Wang, G. Bian, H. Zheng, D. S. Sanchez, I. Belopolski, N. Alidoust, M. Neupane, A. Bansil, H.-T. Jeng, H. Lin, and M. Z. Hasan, Nat. Commun. **7**,10639 (2016).
[34] B. J. Wieder, Y. Kim, A. M. Pappe, and C. L. Kane, Phys. Rev. Lett. **116**, 186402 (2016).
[35] B. Bradlyn, J. Cano, Z. Wang, M. G. Vergniory, C. Felser, R. J. Cava, and B. A. Bernevig, Science **353**, aaf5037 (2016).
[36] G. Chang, S.-Y. Xu, S.-M. Huang, D. S. Sanchez, C.-H. Hsu, G. Bian, Z.-M. Yu, I. Belopolski, N. Alidoust, H. Zheng, T.-R. Chang, H.-T. Jeng, S. A. Yang, T. Neupert, H. Lin, and M. Z. Hasan, Sci. Rep. **7**, 1688 (2017).
[37] H. Weng, C. Fang, Z. Fang, and X. Dai, Phys. Rev. B **93**, 241202 (2016).
[38] Z. Zhu, G. W. Winkler, Q. Wu, J. Li, and A. A. Soluyanov, Phys. Rev. X **6**, 031003 (2016).
[39] G. Chang, S.-Y. Xu, B. J. Wieder, D. S. Sanchez, S.-M. Huang, I. Belopolski, T.-R. Chang, S. Zhang, A. Bansil, H. Lin, and M. Z. Hasan, Phys. Rev. Lett. **119**, 206401 (2017).
[40] P. Tang, Q. Zhou, S.-C. Zhang, Phys. Rev. Lett. **119**, 206402 (2017).
[41] T. Bzdušek, Q. Wu, A. Rüegg, M. Sigrist, and A. A. Soluyanov, Nature **538**, 75 (2016).
[42] G. Chang, S.-Y. Xu, X. Zhou, S.-M. Huang, B. Singh, B. Wang, I. Belopolski, J. Yin, S. Zhang, A. Bansil, H. Lin, and M. Z. Hasan. Phys. Rev. Lett. **119**, 156401 (2017).
[43] F. d. Juan, A. G. Grushin, T. Morimoto, and J. E. Moore, Nat. Commun. **8**, 15995 (2017).
[44] S.-Y. Xu, N. Alidoust, G. Chang, H. Lu, B. Singh, I. Belopolski, D. S. Sanchez, X. Zhang, G. Bian, M.-A. Husanu, Y. Bian, S.-M. Huang, C.-H. Hsu, T.-R. Chang, H.-T. Jeng, A. Bansil, T. Neupert, V. N. Strocov, H. Lin, S. Jia, and M. Z. Hasan, Science Advances **3**, e1603266 (2017).
[45] L. Huang, T. M. McCormick, M. Ochi, Z. Zhao, M.-T. Suzuki, R. Arita, Y. Wu, D. Mou, H. Cao, J. Yan, N. Trivedi, and A. Kaminski, Nat. Mat., **15**, 1155 (2016).
[46] K. Deng, G. Wan, P. Deng, K. Zhang, S. Ding, E. Wang, M. Yan, H. Huang, H. Zhang, Z. Xu, J. Denlinger, A. Fedorov, H. Yang, W. Duan, H. Yao, Y. Wu, S. Fan, H. Zhang, X. Chen, and S. Zhou, Nat. Phys, **12**, 1105 (2016).
[47] I. Belopolski, D. S. Sanchez, Y. Ishida, X. Pan, P. Yu, S.-Y. Xu, G. Chang, T.-R. Chang, H. Zheng, N. Alidoust, G. Bian, M. Neupane, S.-M. Huang, C.-C. Lee, Y. Song, H. Bu, G. Wang, S. Li, G. Eda, H.-T. Jeng, T. Kondo, H. Lin, Z. Liu, F. Song, S. Shin, and M. Z. Hasan, Nat. Commun. **7**, 13643 (2016).
[48] A. Tamai, Q. S. Wu, I. Cucchi, F. Y. Bruno, S. Riccò, T.K. Kim, M. Hoesch, C. Barreteau, E. Giannini, C. Besnard, A.A. Soluyanov, and F. Baumberger. Phys. Rev. X **6**, 031021 (2016).
[49] H. Zheng, G. Bian, G. Chang, H. Lu, S.-Y. Xu, G. Wang, T.-R. Chang, S. Zhang, I. Belopolski, N. Alidoust, D. S. Sanchez, F. Song, H.-T. Jeng, N. Yao, A. Bansil, S. Jia, H. Lin, and M. Z. Hasan, Phys. Rev. Lett. **117**, 266804 (2017).
[50] G. Bian, T.-R. Chang, R. Sankar, S.-Y. Xu, H. Zheng, T. Neupert, C.-K. Chiu, S.-M. Huang, G. Chang, I. Belopolski, D. S. Sanchez, M. Neupane, N. Alidoust, C. Liu, B. Wang, C.-C. Lee, H.-T. Jeng, C. Zhang, Z. Yuan, S. Jia, A. Bansil, F. Chou, H. Lin, and M. Z. Hasan, Nat. Commun, **7**, 10556 (2016).
[51] B. Q. Lv, Z.-L. Feng, Q.-N. Xu, X. Gao, J.-Z. Ma, L.-Y. Kong, P. Richard, Y.-B. Huang, V. N. Strocov, C. Fang, H.-M. Weng, Y.-G. Shi, T. Qian, and H. Ding, Nature **546**, 627 (2017).
[52] G. Xu, H. Weng, Z. Wang, X. Dai, Z. Fang, Phys. Rev. Lett. **107**, 186806 (2011).
[53] M. C. Shapiro, S. C. Riggs, M. B. Stone, C. R. de la Cruz, S. Chi, A. A. Podlesnyak, and I. R. Fisher , Phys. Rev. B **85**, 214434 (2012).
[54] K.-Y. Yang, Y.-M. Lu, Y. Ran, Phys. Rev. B **84**, 075129 (2011).
[55] S. Borisenko, D. Evtushinsky, Q. Gibson, A. Yaresko, T. Kim, M. N. Ali, B. Buechner, M. Hoesch, and R. J. Cava https://arxiv.org/abs/1507.04847 (2015).
[56] A. A. Burkov, Phys. Rev. Lett. **113**, 187202 (2014).
[57] M. Kargarian, M. Randeria, N. Trivedi, Sci. Rep. **5**, 12683 (2015).
[58] A. M. Guloy, J. D. Corbett, Inorg. Chem. **30**, 4789 (1991).
[59] S. K. Dhar, S. M. Corbett, J. Magn. Magn. Mater. **152**, 22 (1996).

[60] E. I. Gladyshevskii, N. Z Nakonechna, K Cenzual, R.EGladyshevskii, J.-LJorda, J Alloys Compd. **296**, 265 (2000).
[61] S. K. Dhar and S. M. Pattalwar, J. Magn. Magn. Mater. **104**, 1303 (1992).
[62] S. Bobev , P. H. Tobash, V. Fritsch, J. D.Thompson, M. F. Hundley, J. L. Sarrao, Z. Fiskc, J. Solid State Chem. **178**, 2091 (2005).
[63] H. Flandorfer, D. Kaczorowski, J. Gröbner, P. Rogl, R. Wouters, C. Godart, A. Kostikas, J. Solid State Chem. **137**, 191 (1998).
[64] J. Wang, B. Lian, S.-C. Zhang, https://arxiv.org/abs/1607.00116 (2016).
[65] S. Murakami, New J. Phys. **9**, 356 (2007).
[66] C.-Z. Chen, J. Song, H. Jiang, Q.-F. Sun, Z. Wang, X. C. Xie, Phys. Rev. Lett. **115**, 246603 (2015).
[67] H. Shapourian, T. L. Hughes, *Phys. Rev. B* **93**, 075108 (2016).
[68] See Supplemental Material for the details of our first-principles electronic calculation methods, energy dispersion and momentum distribution of Weyl fermions in RAlGe family and effective Hamiltonian for W3 nodes.
[69] G. Kresse, D. Joubert, Phys. Rev. B **59**, 1758-1775 (1999).
[70] G. Kresse, J. Furthmller, Comput. Mater. Sci. **6**, 15-50 (1996).
[71] J. P. Perdew, K. Burke, M. Ernzerhof, Phys. Rev. Lett. **77**, 3865-3868 (1996).